Journal of Radioanalytical and Nuclear Chemistry (2023) 332:4889–4896
https://doi.org/10.1007/s10967-023-09197-5

A new fast screening method for estimating building materials hazard indices with correlated inputs

Joanna Rocznik[1,2] · Julia Pluta[1,2] · Konrad Tudyka[1] · Grzegorz Poręba[1] · Agnieszka Szymak[1]

Received: 17 April 2023 / Accepted: 6 October 2023 / Published online: 1 November 2023

Abstract
In this work we investigate a new fast screening method for estimation of chosen hazard indices (*HI*) using correlated inputs dedicated for small 3.00 g samples using a novel µDOSE. The system detects α and β particles separately, along with ^{220}Rn/^{216}Po, ^{219}Rn/^{215}Po, ^{212}Bi/^{212}Po and ^{214}Bi/^{214}Po decay pairs. Four separate decay pairs along with α and β particle count rates are used to quantify decay chains. The excess β count rates is used to quantify the ^{40}K radioactivity. This provides radionuclide estimates that are correlated—and this correlation is taken into account in calculating hazard indices with their corresponding uncertainties. Calculated hazard indices are verified against state-of-the-art High Resolution Gamma Spectrometry (HRGS) equipped with a High Purity Germanium (HPGe) detector manufactured by Canberra. This research shows that results obtained with the µDOSE system correspond to the results obtained with HRGS and when the activity correlation is taken into account the *HI* uncertainties are similar in value for both methods.

Keywords Building materials · Natural radioactivity · Correlated uncertainties · α and β counting · Building materials hazard indices

Introduction

Building materials are derived from Earth's resources, such as soil or rocks, and thus they contain naturally occurring radionuclides from the ^{238}U and ^{232}Th decay series, as well as ^{40}K and, as a result, their use carries a risk of radiation exposure. This exposure can be external from direct gamma radiation exposure or internal from inhalation of radioactive radon/thoron [1]. The latter can be especially harmful in an indoor environment and can contribute to development of lung cancer, if there is no appropriate ventilation [2]. For this reason a number of regulations have been introduced providing so-called hazard indices. For example, to ensure safety regarding the dose acquired exclusively from building materials, activity concentration index value of 1 can be used as a conservative screening tool [3]. Similar mathematical formulation can be seen in other hazard indices, namely: radium equivalent activity, representative level index, absorbed and annual gamma dose rates, respectively, gamma effective indices, as well as external and internal radiation hazard indices.

The issue of building materials radioactivity is well documented in various works, as listed in Table 1. However, because the µDOSE system is a relatively new setup for estimating ^{40}K as well as ^{238}U, ^{235}U and ^{232}Th decay chain members activities [4], no research on hazard indices has been done so far. A 2022 study [5] on the accuracy of the µDOSE system shows good agreement with well-established methods of dosimetry, such as HRGS or thick source alpha counting. The study also mentions that the correlation of results provided by the µDOSE system improves precision of dose rate estimation; however, this correlation has not been investigated on its own and nor has its significance in comparison to the HRGS method.

The aim of this work is to test how uncertainties of hazard indices are influenced, if radionuclide estimates are correlated. This is tested with two independent setups of HRGS and the µDOSE system that provide uncorrelated and correlated estimates respectively. In addition, advantages of reducing hazard indices uncertainties are investigated by

✉ Joanna Rocznik
joanna.rocznik@polsl.pl

[1] Institute of Physics – Centre for Science and Education, Silesian University of Technology, ul. Konarskiego 22B, 44-100 Gliwice, Poland

[2] miDose Solutions, ul. Wolności 234b/4, 41-800 Zabrze, Poland

using correlated radionuclide estimates and drawbacks as errors are induced by disequilibrium in radioactive decay chains.

Experimental

Materials

All 7 samples that were investigated in this work are frequently used building materials of known origin: clay bricks (SiO_2, feldspars), beach rock (sand and/or gravel, $CaCO_3$) and sand (SiO_2). Samples were dried in a drying chamber at an elevated temperature of 80 °C for several days. During drying sample masses were monitored to ensure water was removed. Every sample material was divided into two subsamples for µDOSE and HRGS measurement. Detailed descriptions of sample preparation for these systems is provided below.

Subsamples and reference materials for µDOSE system measurements were ground in a Fritsch Pulverisette 6 planetary mill for 45 min at 200 rpm each to a fine powder, then 3.00 g of prepared material was placed onto 70 mm diameter sample discs and measured using the µDOSE system.

Subsamples and reference materials for HRGS measurements were put and sealed in γBEAKERS [21, 22] (ca. 100 g samples) and then stored for a period of about 30 days to obtain secular equilibrium to avoid bias that arises from ^{222}Rn emanation [23–27]. Subsamples were measured for 24–48 h, times varying depending on the activities of each individual sample for obtaining optimal count rate statistics.

µDOSE system—α/β and delayed coincidence counting

For α/β particle measurements µDOSE system was used, described in detail in [4, 5]. It is designed for detecting α-α (^{220}Rn/^{216}Po, ^{219}Rn/^{215}Po) and β-α (^{212}Bi/^{212}Po, ^{214}Bi/^{214}Po) decay pairs and identifying the isotope pair the particles come from, based on the characteristic time intervals between the subsequent particle emissions. These pairs can later be used to determine ^{238}U, ^{235}U, ^{232}Th and ^{40}K content. This is done with assumption of secular equilibrium, where the activities of the decay pairs are equal to the activities of corresponding decay chains parent radioisotopes: ^{238}U, ^{235}U or ^{232}Th. The remainder of the emitted β particles are assigned to ^{40}K. The system was calibrated using IAEA-RGU-1, IAEA-RGTh-1 and IAEA-RGK-1 [28] reference materials obtained from the International Atomic Energy Agency. In this work a system that was calibrated for 3.00 g was used.

Background activity was obtained for a 3.00 g background plastic disc placed accordingly in the sample holder. The background measurement lasted ca. 48 h and was performed in the same laboratory conditions as were the samples.

High resolution gamma spectrometry

Gamma spectrometry was performed with a Canberra HPGe detector with FWHM of 1.8 keV and relative efficiency 40% at 1332 keV. The HRGS system was calibrated with IAEA-RGU-1, IAEA-RGTh-1 and IAEA-RGK-1 [28] reference materials. Activities were calculated for selected energy lines: 295.2 keV, 351.9 keV (^{214}Pb) and 609.3 keV (^{214}Bi) for uranium series; 338.3 keV, 911.2 keV (^{228}Ac) and 583.2 keV (^{208}Tl) for thorium series; and 1460.8 keV (^{40}K) (data obtained from NuDat 3.0).

Background activity was obtained through a 167 h measurement of an empty γBEAKER in an identical laboratory setting in which samples were measured.

Theoretical

Radiation hazard indices

To determine whether building materials meet set standards, are within established norms and are safe to use, a number of hazard indices were devised. In many cases hazard indices are estimated from ^{226}Ra, ^{232}Th and ^{40}K concentrations and provide a simplified information for a given risk factor. Frequently used indices are calculated as a linear combination of ^{226}Ra, ^{232}Th and ^{40}K radionuclides contents in the following way:

$$HI = S_{\mathrm{Ra}}A_{\mathrm{Ra}} + S_{\mathrm{Th}}A_{\mathrm{Th}} + S_{\mathrm{K}}A_{\mathrm{K}} \quad (1)$$

where HI is the hazard index, A_{Ra}, A_{Th} and A_{K} are ^{226}Ra, ^{232}Th and ^{40}K concentrations expressed in Bq·kg^{-1} respectively, S_{Ra}, S_{Th} and S_{K} are parameters for a given hazard index. List of hazard indices, S_{Ra}, S_{Th}, S_{K} parameters and a brief summary is provided in Table 1.

Uncertainty propagation for uncorrelated and correlated inputs

For uncorrelated inputs given hazard index uncertainty (σ_{Th}) can be is calculated as:

$$\sigma_{HI}^2 = (S_{\mathrm{Ra}}\sigma_{\mathrm{Ra}})^2 + (S_{\mathrm{Th}}\sigma_{\mathrm{Th}})^2 + (S_{\mathrm{K}}\sigma_{\mathrm{K}})^2 \quad (2)$$

where σ_{Ra}, σ_{Th} and σ_K are uncertainties of ^{226}Ra, ^{232}Th and ^{40}K activities. Usually HRGS measurements are considered to be uncorrelated. However for correlated inputs hazard index uncertainty should be calculated using the formula that takes into account correlations:

$$\sigma_{HI}^2 = \begin{bmatrix} S_{Ra} & S_{Th} & S_K \end{bmatrix} \begin{bmatrix} \sigma_{Ra}^2 & \sigma_{Ra-Th} & \sigma_{Ra-K} \\ \sigma_{Th-Ra} & \sigma_{Th}^2 & \sigma_{Th-K} \\ \sigma_{K-Ra} & \sigma_{K-Th} & \sigma_K^2 \end{bmatrix} \begin{bmatrix} S_{Ra} \\ S_{Th} \\ S_K \end{bmatrix} \quad (3)$$

where non-diagonal σ elements are covariances of elements given in subscripts. Depending on sign and value of non-diagonal elements the final *HI* uncertainty will give different values. For uncorrelated inputs non diagonal σ are zeros and Eqs. 2 and 3 provide the same values.

Results and discussion

Correlated ^{226}Ra, ^{232}Th and ^{40}K estimates

The µDOSE system provides correlated ^{226}Ra, ^{232}Th and ^{40}K estimates. This arises because the system detects α particles that can be emitted from decay chains while β particles are emitted from decay chains and ^{40}K. Four decay pairs ^{220}Rn/^{216}Po, ^{219}Rn/^{215}Po, ^{212}Bi/^{212}Po, ^{214}Bi/^{214}Po detected by the µDOSE system, provide information on relative ^{226}Ra, ^{232}Th and ^{40}K content. Detailed calculation procedure is provided in [29]. Correlations of ^{226}Ra, ^{232}Th and ^{40}K contents are visualised in Fig. 1 where 100 k points were drawn with respect to correlations determined by α, β and four decay pairs counting statistics.

Table 1 Radiation hazard indices; names, parameters and descriptions of 7 hazard indices, along with references to other works where the indices were studied

HI—Hazard index	S_{Ra}	S_{Th}	S_K	Short description	References
Radium equivalent activity (Ra_{eq})	1	1.43	0.077	Radium equivalent activity Ra_{eq} helps determine the purpose a given building material can be used for, e.g. homes, industries, roads/bridges, foundations of non-residential constructions or whether it is not suitable for any type of construction use at all	[6–17]
Representative level index (*RLI*)	150^{-1}	100^{-1}	1500^{-1}	Representative level index *RLI* allows for estimating gamma radiation levels associated with concentrations of specific nuclides	[7–10, 12, 16]
Absorbed gamma dose (D_r in nGy·h^{-1})	0.92	1.1	0.08	Absorbed gamma dose rate D_R is a value dependent on "average" room parameters (4×5×2.8 m) with wall and ceiling thickness at 20 cm and their density of 2 350 kg·m^{-3} (for concrete)	[8, 10, 12, 14, 17, 18]
Annual effective dose rate* (H_R in mSv·a^{-1})	$1.13 \cdot 10^{-3}$	$1.13 \cdot 10^{-3}$	$9.82 \cdot 10^{-5}$	Annual effective dose rate H_R is a parameter dependent on the absorbed gamma dose rate multiplied by a conversion factor (0.7 Sv·Gy^{-1}) and outdoor occupancy factor (0.2)	[8, 10, 12]
Activity concentration index	300^{-1}	200^{-1}	3000^{-1}	Presented in the form proposed by the European Commission, the value of I_γ is an indicator if material in use exceeds the established safety levels that depend on the dose criterion and the type of use as well as the amount of material	[6, 8, 10, 12, 14–20]
External radiation hazard index	370^{-1}	258^{-1}	4810^{-1}	Both internal (H_{in}) and external (H_{ex}) radiation hazard index has a function similar to the activity concentration index, but they take into account the way radiation interacts with the human body (inhalation or external influence)	[7–10, 12, 13, 15, 16, 18]
Internal radiation hazard index	185^{-1}	259^{-1}	4810^{-1}		

Parameters are applicable for radionuclides concentrations expressed in Bq·kg^{-1}

*Usually presented as: $H_R = D_R \cdot 8\,766 \cdot 0.2 \cdot 0.7 \cdot 10^{-6}$

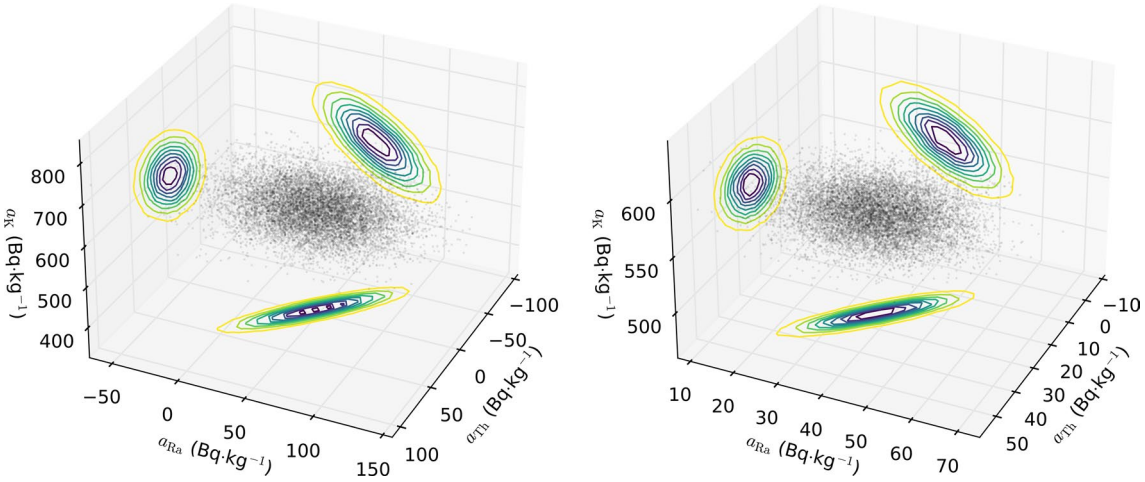

Fig. 1 Two ^{226}Ra, ^{232}Th and ^{40}K compositions. Isolines are showing projected 2-D PDF contour-plots drawn from a multivariate normal distribution for the μDOSE system for 1 h (**a**) and 10 h (**b**) measurements

Table 2 Numerical data of ^{226}Ra, ^{232}Th and ^{40}K radionuclides contents from μDOSE and HRGS

Sample number	μDOSE $\left[\mu_{\text{Ra-226}}\ \ \mu_{\text{Th-232}}\ \ \mu_{K-40}\right]$ terms in Bq·kg^{-1} each	$\begin{bmatrix}\sigma^2_{\text{Ra-226}} & \sigma_{\text{Ra-226, Th-232}} & \sigma_{\text{Ra-226, K-40}}\\ \sigma_{\text{Th-232, Ra-226}} & \sigma^2_{\text{Th-232}} & \sigma_{\text{Th-232, K-40}}\\ \sigma_{\text{K-40, Ra-226}} & \sigma_{\text{K-40, Th-232}} & \sigma^2_{\text{K-40}}\end{bmatrix}$ terms in Bq^2·kg^{-2} each	HRGS ^{226}Ra, Bq·kg^{-1}	^{232}Th, Bq·kg^{-1}	^{40}K, Bq·kg^{-1}
1	[29.83 18.56 639.35]	$\begin{bmatrix}47.15 & -38.82 & 35.77\\ -38.82 & 34.92 & -38.56\\ 35.77 & -38.56 & 724.39\end{bmatrix}$	25.21 ± 0.89	23.4 ± 1.7	446 ± 22
2	[36.42 24.17 500.63]	$\begin{bmatrix}55.81 & -46.63 & 44.42\\ -46.63 & 41.69 & -45.52\\ 44.42 & -45.52 & 601.58\end{bmatrix}$	25.55 ± 0.89	28.8 ± 2.0	469.0 ± 22.7
3	[33.20 31.11 772.12]	$\begin{bmatrix}45.74 & -37.99 & 35.73\\ -37.99 & 34.40 & -38.42\\ 35.73 & -38.42 & 804.74\end{bmatrix}$	28.4 ± 1.6	36.9 ± 2.8	513 ± 44
4	[1.39 0.28 204.49]	$\begin{bmatrix}0.59 & -0.12 & -0.85\\ -0.12 & 0.16 & -0.31\\ -0.85 & -0.31 & 194.19\end{bmatrix}$	2.66 ± 0.17	3.00 ± 0.29	106.9 ± 8.4
5	[0.0 4.77 179.01]	$\begin{bmatrix}6.65 & -4.75 & 2.90\\ -4.75 & 3.94 & -4.11\\ 2.90 & -4.11 & 196.24\end{bmatrix}$	3.64 ± 0.24	3.68 ± 0.35	80.0 ± 6.7
6	[0.59 1.88 0.0]	$\begin{bmatrix}0.83 & -0.44 & -0.20\\ -0.44 & 0.56 & -1.10\\ -0.20 & -1.10 & 160.78\end{bmatrix}$	4.93 ± 0.26	4.06 ± 0.41	−5.1 ± 2.3
7	[33.80 28.06 567.43]	$\begin{bmatrix}20.30 & -19.73 & 24.85\\ -19.73 & 22.78 & -33.20\\ 24.85 & -33.20 & 228.52\end{bmatrix}$	27.90 ± 0.86	33.9 ± 2.1	525 ± 24

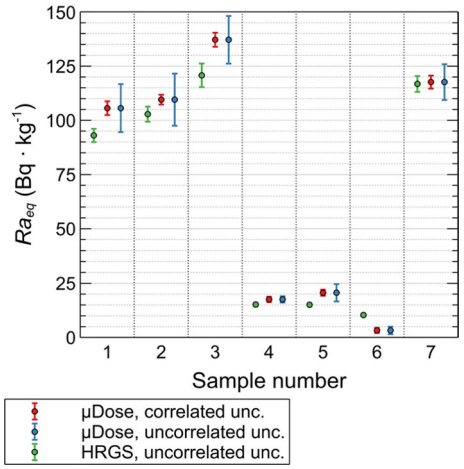

Fig. 2 Radium equivalent activity (Ra_{eq}) with uncertainties calculated for all samples

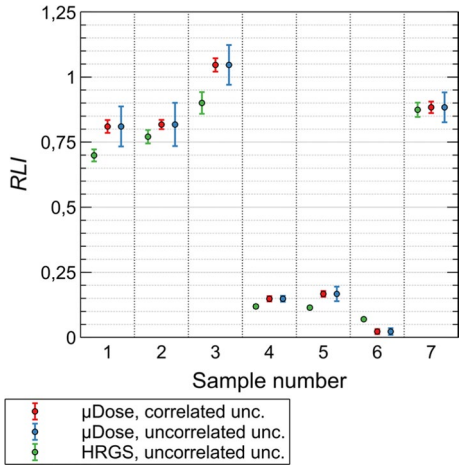

Fig. 3 Representative level index (*RLI*) with uncertainties calculated for all samples

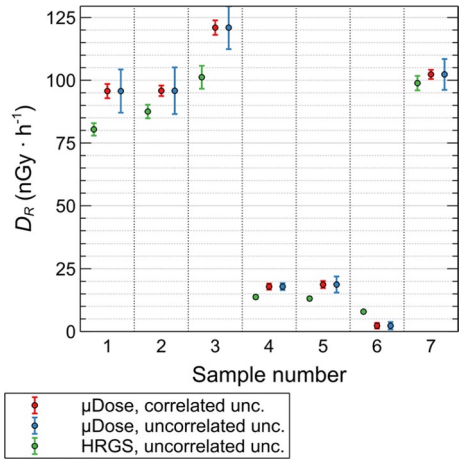

Fig. 4 Absorbed gamma dose (D_R) with uncertainties calculated for all samples

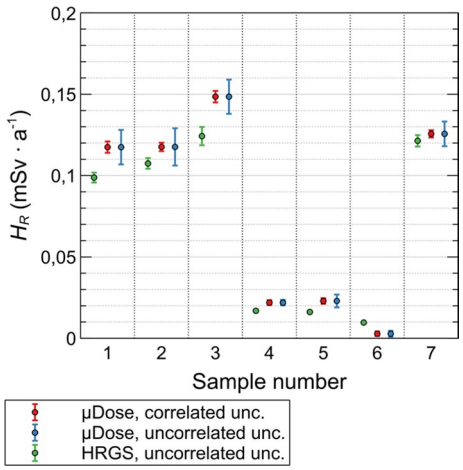

Fig. 5 Annual effective dose rate (H_R) with uncertainties calculated for all samples

Hazard indices and their uncertainties

Hazard indices and their uncertainties were estimated for the μDOSE system and HRGS using radionuclide content. Numerical values are provided in Table 2. In the case of the μDOSE system uncertainties are calculated using two approaches: first neglects correlations (Eq. 2) and the second approach takes correlations into account (Eq. 3). This is illustrated on Figs. 2, 3, 4, 5, 6, 7 and 8 which provide comparison of hazard indices values and their uncertainties.

Data presented in Figs. 2, 3, 4, 5, 6, 7 and 8 shows that the uncorrelated uncertainties for μDOSE measurements are greater than the correlated uncertainties. This shows that by including the correlation between the activities of ^{226}Ra, ^{232}Th and ^{40}K in the estimation of hazard indices uncertainties, the provided results are more precise. This is due to the fact that several elements within the covariance matrices (Eq. 3) are negative which contributes to the lessening of the uncertainties. The correlated uncertainties from μDOSE measurements are also similar in value to the ones obtained from HRGS, thus proving that the measurement accuracy is maintained regardless of the chosen method.

Screening—measurement time, uncertainty and type II error

In some cases sample mass and sample throughput can be a limiting factor; therefore, an investigation on how uncertainty changes as a function of time was performed. The μDOSE system offers the possibility of measuring small samples and in this work the system was calibrated

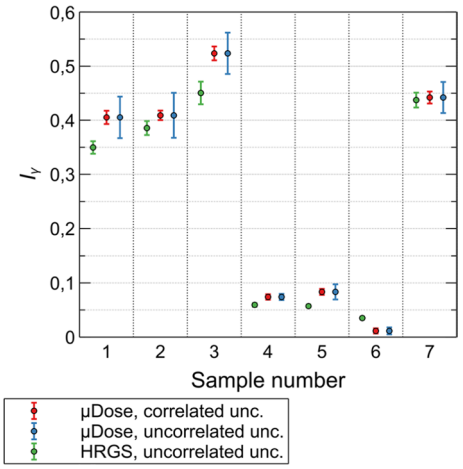

Fig. 6 Activity concentration index I_γ with uncertainties calculated for all samples

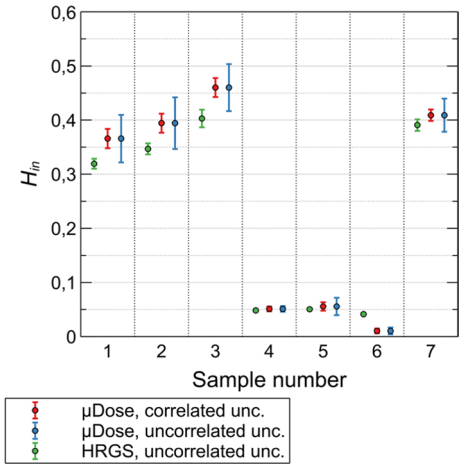

Fig. 8 Internal radiation hazard index (H_{in}) with uncertainties calculated for all samples

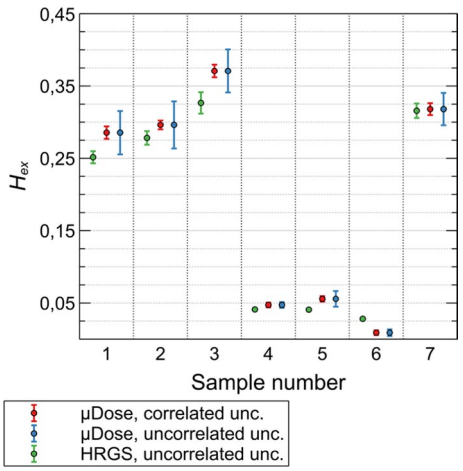

Fig. 7 External radiation hazard index (H_{ex}) with uncertainties calculated for all samples

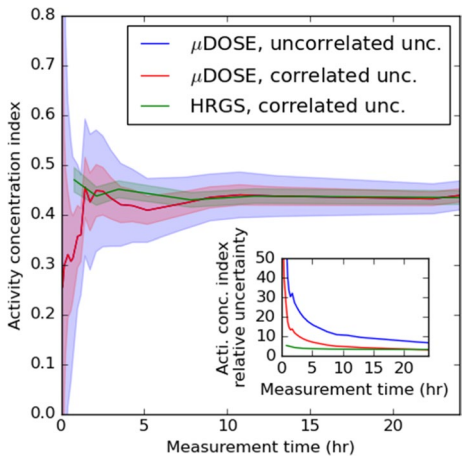

Fig. 9 Activity concentration index value uncertainty as a function of measurement time for HRGS (100 g samples) and μDOSE system (3.00 g samples)

for 3.00 g samples, whereas HRGS was calibrated for 100 g. Figure 9 shows activity concentration index value and uncertainty as a function of measurement time for HRGS and μDOSE system. In both cases uncertainties encompass counting statistics, sample mass and reference materials uncertainties which are the main uncertainty contributors for prolonged measurements. Despite large mass differences, μDOSE uncertainties that take into account correlations are comparable with HRGS (Fig. 9). For the first few hours of the measurement activity concentration index uncertainty is relatively large for μDOSE. After 10 h (Fig. 9) uncertainties from the μDOSE and HRGS systems are at the same level, which further proves that the μDOSE system is a reliable screening tool and can be an alternative to conventional HRGS. Nevertheless, algorithms that are used for measuring net peak area do not operate well on poorly defined baseline and therefore first peak quantification, used for activity estimation, was available after 46 min of measurements and required manually adjusting regions for peak detection.

In case of screening building materials for activity concentration index (Fig. 9) it can be observed that after ca. 1 h of measurement its value is well below recommended value 1 [3]. For shorter measurements HRGS counting statistics (discussed in the paragraph above) and μDOSE counting statistics do not provide definitive material classification. This finding has substantial implications for future studies, especially when sample mass or measurement time is a limiting factor. What is more, understanding the differences between

correlated and uncorrelated uncertainties allows researchers to take advantage of correlated ones.

While screening *HI* there are two classification errors: type I error "false positive" and type II error "false negative". If *HI* value is above threshold, additional and prolonged measurement should be made to resolve this. In case of type II error, this can be difficult to detect and can have more significant consequences. For example, given *HI* can falsely be assumed to be within limits. This can happen because there are several factors, not related to counting statistics, that contribute to this. For example ^{238}U decay chain can be in disequilibrium, [25, 30, 31] or sample chemical composition can be unknown. This can cause issues in both HRGS as well as in the µDOSE system and unfortunately those factors are not controlled routinely due to cost of additional measurements. Nevertheless, *HI* screening limits can be set to reduce the risk of type II errors at the expense of type I error.

The proposed methodology and obtained findings allow to bridge a gap in the existing literature, especially in the context of improving the throughput with measurement systems like µDOSE. The precision of conducted measurements ensures that safety thresholds are reliably met, reducing risks associated with type I and II errors.

Conclusions

In this study, values of selected hazard indices of building materials were compared using the µDOSE system for 3.00 g samples against the HRGS calibrated for 100 g samples. The primary objective was to understand the significance of the correlation of activities of ^{226}Ra, ^{232}Th, and ^{40}K provided uniquely by the µDOSE system. The findings indicated that the uncertainties in hazard indices from both the HRGS and µDOSE systems, when correlations are considered, are comparable in value. Furthermore, accounting for these correlations offers a substantial enhancement in the precision of results compared to when they are disregarded.

Acknowledgements This research was a part of Project-Based Learning (PBL) and was co-funded by the Silesian University of Technology Excellence Initiative – Research University (Gliwice, Poland). The presented results were obtained with the support of the Polish National Science Centre, contract number: 2021/41/N/ST10/00169.

Author contributions JR: Conceptualization, Methodology, Formal analysis, Investigation, Writing—Original Draft; JP: Conceptualization, Methodology, Formal analysis, Investigation, Writing—Original Draft; KT: Conceptualization, Methodology, Formal analysis, Investigation, Writing—Original Draft, Supervision; GP: Conceptualization, Methodology, Formal analysis, Investigation, Writing—Original Draft, Supervision; AS: Investigation.

Declarations

Conflict of interest The authors declare that they have no known competing financial interests or personal relationships that could have appeared to influence the work reported in this paper.

References

1. European Commission (1999) Radiation protection 112 radiological protection principles concerning the natural radioactivity of building materials. https://ec.europa.eu/energy/sites/ener/files/documents/112.pdf
2. Chen J, Rahman NM, Atiya IA (2010) Radon exhalation from building materials for decorative use. J Environ Radioact 101:317–322. https://doi.org/10.1016/j.jenvrad.2010.01.005
3. The Council of European Union (2013) Council directive 2013/59/Euratom of 5 December 2013. https://eur-lex.europa.eu/legal-content/EN/TXT/PDF/?uri=CELEX:32013L0059&from=EN
4. Tudyka K, Miłosz S, Adamiec G, Bluszcz A, Poręba G, Paszkowski Ł, Kolarczyk A (2018) µDOSE: a compact system for environmental radioactivity and dose rate measurement. Radiat Meas 118:8–13. https://doi.org/10.1016/j.radmeas.2018.07.016
5. Kolb T, Tudyka K, Kadereit A, Lomax J, Poręba G, Zander A, Zipf L, Fuchs M (2022) The µDOSE system: determination of environmental dose rates by combined alpha and beta counting—performance tests and practical experiences. Geochronology 4:1–31. https://doi.org/10.5194/gchron-4-1-2022
6. Devi V, Kumar A, Chauhan RP (2019) A study on radionuclides content and radon exhalation from soil of Northern India. Environ Earth Sci 78:506. https://doi.org/10.1007/s12665-019-8512-9
7. Thabayneh KM, Jazzar MM (2012) Natural radioactivity levels and estimation of radiation exposure in environmental soil samples from Tulkarem Province–Palestine, open. J Soil Sci 02:7–16. https://doi.org/10.4236/ojss.2012.21002
8. Mann N, Kumar A, Kumar S, Chauhan RP (2018) Measurement of radium, thorium, potassium and associated hazard indices from the soil samples collected from Northern India. Indoor Built Environ 27:1149–1156. https://doi.org/10.1177/1420326X17696136
9. Beretka J, Matthew PJ (1985) Natural radioactivity of Australian building materials, industrial wastes and by-products. Health Phys 48:87–95. https://doi.org/10.1097/00004032-198501000-00007
10. Ravisankar R, Vanasundari K, Suganya M, Raghu Y, Rajalakshmi A, Chandrasekaran A, Sivakumar S, Chandramohan J, Vijayagopal P, Venkatraman B (2014) Multivariate statistical analysis of radiological data of building materials used in Tiruvannamalai, Tamilnadu, India. Appl Radiat Isot 85:114–127. https://doi.org/10.1016/j.apradiso.2013.12.005

11. Hassan NM, Ishikawa T, Hosoda M, Sorimachi A, Tokonami S, Fukushi M, Sahoo SK (2010) Assessment of the natural radioactivity using two techniques for the measurement of radionuclide concentration in building materials used in Japan. J Radioanal Nucl Chem 283:15–21. https://doi.org/10.1007/s10967-009-0050-6
12. Turhan Ş (2008) Assessment of the natural radioactivity and radiological hazards in Turkish cement and its raw materials. J Environ Radioact 99:404–414. https://doi.org/10.1016/j.jenvrad.2007.11.001
13. Ravisankar R, Vanasundari K, Chandrasekaran A, Rajalakshmi A, Suganya M, Vijayagopal P, Meenakshisundaram V (2012) Measurement of natural radioactivity in building materials of Namakkal, Tamil Nadu, India using gamma-ray spectrometry. Appl Radiat Isot 70:699–704. https://doi.org/10.1016/j.apradiso.2011.12.001
14. Ravisankar R, Raghu Y, Chandrasekaran A, Suresh Gandhi M, Vijayagopal P, Venkatraman B (2016) Determination of natural radioactivity and the associated radiation hazards in building materials used in Polur, Tiruvannamalai District, Tamilnadu, India using gamma ray spectrometry with statistical approach. J Geochem Explor 163:41–52. https://doi.org/10.1016/j.gexplo.2016.01.013
15. Turhan Ş, Baykan UN, Şen K (2008) Measurement of the natural radioactivity in building materials used in Ankara and assessment of external doses. J Radiol Prot 28:83–91. https://doi.org/10.1088/0952-4746/28/1/005
16. Eštoková A, Palaščáková L (2013) Assessment of natural radioactivity levels of cements and cement composites in the Slovak Republic. Int J Environ Res Public Health 10:7165–7179. https://doi.org/10.3390/ijerph10127165
17. Nuccetelli C, Risica S, D'Alessandro M, Trevisi R (2012) Natural radioactivity in building material in the European Union: robustness of the activity concentration index *I* and comparison with a room model. J Radiol Prot 32:349–358. https://doi.org/10.1088/0952-4746/32/3/349
18. Damla N, Cevik U, Kobya AI, Celik A, Celik N, Van Grieken R (2010) Radiation dose estimation and mass attenuation coefficients of cement samples used in Turkey. J Hazard Mater 176:644–649. https://doi.org/10.1016/j.jhazmat.2009.11.080
19. Trevisi R, Risica S, D'Alessandro M, Paradiso D, Nuccetelli C (2012) Natural radioactivity in building materials in the European Union: a database and an estimate of radiological significance. J Environ Radioact 105:11–20. https://doi.org/10.1016/j.jenvrad.2011.10.001
20. Righi S, Bruzzi L (2006) Natural radioactivity and radon exhalation in building materials used in Italian dwellings. J Environ Radioact 88:158–170. https://doi.org/10.1016/j.jenvrad.2006.01.009
21. Poręba G, Tudyka K, Walencik-Łata A, Kolarczyk A (2020) Bias in 238U decay chain members measured by γ-ray spectrometry due to 222Rn leakage. Appl Radiat Isot 156:108945. https://doi.org/10.1016/j.apradiso.2019.108945
22. Tudyka K, Poręba G, Szymak A, Rocznik J, Pluta J, Schüler T, Kolb T, Murray A (2021) Systematic error in 238U decay chain radionuclides measurements due to 222Rn emanation from reference materials. Measurement 184:109893. https://doi.org/10.1016/j.measurement.2021.109893
23. Markkanen M, Arvela H (1992) Radon emanation from soils. Radiat Prot Dosim 45:269–272. https://doi.org/10.1093/rpd/45.1-4.269
24. Sakoda A, Ishimori Y, Yamaoka K (2011) A comprehensive review of radon emanation measurements for mineral, rock, soil, mill tailing and fly ash. Appl Radiat Isot 69:1422–1435. https://doi.org/10.1016/j.apradiso.2011.06.009
25. Sakoda A, Nishiyama Y, Hanamoto K, Ishimori Y, Yamamoto Y, Kataoka T, Kawabe A, Yamaoka K (2010) Differences of natural radioactivity and radon emanation fraction among constituent minerals of rock or soil. Appl Radiat Isot 68:1180–1184. https://doi.org/10.1016/j.apradiso.2009.12.036
26. Seo BK, Lee KY, Yoon YY, Lee DW (2001) Direct and precise determination of environmental radionuclides in solid materials using a modified Marinelli beaker and a HPGe detector. Fresenius J Anal Chem 370:264–269. https://doi.org/10.1007/s002160000695
27. Bonczyk M, Samolej K (2019) Testing of the radon tightness of beakers and different types of sealing used in gamma-ray spectrometry for 226Ra concentration determination in NORM. J Environ Radioact 205–206:55–60. https://doi.org/10.1016/j.jenvrad.2019.05.007
28. IAEA (1987) IAEA/RL/148. In: International atomic energy agency, Vienna
29. Tudyka K, Bluszcz A, Poręba G, Miłosz S, Adamiec G, Kolarczyk A, Kolb T, Lomax J, Fuchs M (2020) Increased dose rate precision in combined α and β counting in the μDOSE system: a probabilistic approach to data analysis. Radiat Meas 134:106310. https://doi.org/10.1016/j.radmeas.2020.106310
30. Bonczyk M (2023) The behavior of the 210Pb during the recycling of selected waste in the metallurgical industry. Appl Radiat Isot 191:110563. https://doi.org/10.1016/j.apradiso.2022.110563
31. Michalik B, Wysocka M, Bonczyk M, Samolej K, Chmielewska I (2020) Long term behaviour of radium rich deposits in a lake ecosystem. J Environ Radioact 222:106349. https://doi.org/10.1016/j.jenvrad.2020.106349